where $\omega_{1\,\mathrm{nom}}(t)$, $\omega_{2\,\mathrm{nom}}(t)$, and $\omega_{3\,\mathrm{nom}}(t)$ are the nominal angular rates, which can be determined by the procedure described by Eq. (5); and $-H_{sz}\omega_{3\,\mathrm{nom}}(t)$, $-H_{sx}\omega_{1\,\mathrm{nom}}(t)$, and $-H_{sy}\omega_{2\,\mathrm{nom}}(t)$ are the reaction torques from the torquers of the gyros. Following the derivation of Eq. (16), the integration of Eqs. (17–19) gives the three angular velocity components:

$$\omega_1(t) = \omega_{1\,\mathrm{nom}}(t) - (H_{sx}/I_1)[\delta_x(t) - \delta_x(t - T_s)] \quad (20)$$

$$\omega_2(t) = \omega_{2\,\mathrm{nom}}(t) - (H_{sy}/I_2)[\delta_y(t) - \delta_y(t - T_s)] \quad (21)$$

$$\omega_3(t) = \omega_{3\,\mathrm{nom}}(t) - (H_{sz}/I_3)[\delta_z(t) - \delta_z(t - T_s)] \quad (22)$$

Accuracy Analysis of the AMG

As indicated in Eq. (16), the output of the AMG satisfies $\delta(t) - \delta(t - T_s) = (-I_1/H_s)[\omega_1(t) - \omega_{1\,\mathrm{nom}}(t)]$. If the ratio I_1/H_s is large, then the minimum angular velocity that the AMG is able to sense may be small, which means that the AMG could improve the accuracy of the usual closed-loop gyro.

Consider an example as follows: The spacecraft's moment of inertia is $I_1 = 10^3$ N-m-s^2. The angular momentum of the gyro is $H_s = 1.05$ N-m-s, the maximum angular rate of the gyro is $\omega_{1\,\max} = 1$ deg/s, and the sample frequency of the gyro is $f_s = 2$ Hz. The pulse frequency of the gyro is $f_q < 2(10^4)$ Hz. (For some gyros $\omega_{1\,\max}/f_q = 0.001$ is a typical value.) Then Eqs. (6) and (16) imply that the closed-loop gyro is not able to sense the angular rate of 10^{-4} deg/s, but the AMG is able to sense the angular rate of 10^{-4} deg/s if the scale error of the gimbal precession angle is 0.1 deg.

Conclusions

The usual closed-loop RIG operates on the moment relationship along the gyro's output axis, and its accuracy depends on the current pulse frequency. The AMG proposed in this Note utilizes the moment relationship along the input axis. It is shown that the AMG directly senses the spacecraft's angular momentum instead of the angular rate through the gimbal precession angle and that the AMG is capable of improving the accuracy of the usual closed-loop gyro provided that the spacecraft's moment of inertia is large.

Acknowledgments

The author would like to thank the editors and the reviewers of this Note for their constructive comments.

References

[1]Shmuel, M., *Aerospace Sensor Systems and Applications*, Springer–Verlag, New York, 1996, pp. 15–200.

[2]Wertz, J. R., *Spacecraft Attitude Determination and Control*, Kluwer Academic, Norwell, MA, 1978, pp. 196–203.

[3]Lawrence, A., *Modern Inertial Technology, Navigation, Guidance, and Control*, Springer–Verlag, New York, 1993, pp. 1–55.

[4]Gary, S. C., Morrow, L. D., and Mamen, R., "Strapdown Navigation Technology: A Literature Survey," *Journal of Guidance and Control*, Vol. 1, No. 3, 1978, pp. 161–172.

[5]Oconnor, B. J., "A Description of the CMG and Its Application to Space Vehicle Control," *Journal of Spacecraft and Rockets*, Vol. 6, No. 3, 1969, pp. 225–231.

[6]Jacot, A. D., "Control Moment Gyros in Attitude Control," *Journal of Spacecraft and Rockets*, Vol. 3, No. 10, 1966, pp. 1313–1320.

[7]Cilburn, B., "Computational Consideration for a Spacecraft Attitude Control System Employing Control Moment Gyros," *Journal of Spacecraft and Rockets*, Vol. 14, No. 1, 1977, pp. 45–53.

[8]Zhang, C., and He, C., *Inertial Technology*, Science Press of China, Beijing, 1987, pp. 31–84.

C. A. Kluever
Associate Editor

Fabrication and Testing of a Leading-Edge-Shaped Heat Pipe

David E. Glass*
Analytical Services and Materials, Inc., Hampton, Virginia 23666
Charles J. Camarda†
NASA Johnson Space Center, Houston, Texas 77058
and
Michael A. Merrigan,§ J. Tom Sena,‡ and Robert S. Reid‡
Los Alamos National Laboratory, Los Alamos, New Mexico 87545

Introduction

STAGNATION regions, such as wing and tail leading edges and nose caps, are critical design areas of hypersonic aerospace vehicles because of the hostile thermal environment those regions experience during flight. As a hypersonic vehicle travels through the Earth's atmosphere, the high local heating and aerodynamic forces cause very high temperatures, severe thermal gradients, and high stresses. Analytical studies and laboratory and wind-tunnel tests indicate that a solution to the thermal–structural problems associated with stagnation regions of hypersonic aerospace vehicles might be obtained by the use of heat pipes to cool these regions.

Preliminary design studies at NASA Langley Research Center (LaRC) indicate that a refractory-composite/refractory-metal heat-pipe-cooled leading edge can reduce the leading-edge mass by over 50% compared to an actively cooled leading edge, can completely eliminate the need for active cooling, and has the potential to provide failsafe and redundant features.[1] Recent work to develop this novel refractory-composite/refractory-metal heat-pipe-cooled leading edge for hypersonic vehicles combines advanced high-temperature materials, coatings, and fabrication techniques with an innovative thermal–structural design. Testing of a component at NASA LaRC with three straight molybdenum–rhenium (Mo–Re) heat pipes embedded in carbon/carbon (C/C) has demonstrated the feasibility of operating heat pipes embedded in C/C (Ref. 2). In those tests, the heat pipes were tested with quartz lamps up to temperatures near 2200°F. Some of the key concepts utilized in the fabrication of the refractory-composite heat-pipe-cooled leading edge, such as a compliant or removable layer to reduce thermal stresses and a slightly convex surface to maintain good thermal contact, have been patented.[3]

The present Note discusses the next step in the development of a refractory-composite/refractory-metal heat-pipe-cooled leading edge: a leading-edge-shaped heat pipe with a relatively sharp leading edge and a thin wall thickness. (More details of this work may be found in Ref. 4.) Numerous fabrication issues were resolved in the fabrication of both the heat-pipe container and wick. The heat pipe was fabricated from arc cast Mo–41Re, used lithium as the working fluid, and had a D-shaped cross section and a 400 × 400 mesh Mo–5Re screen wick with a single artery along the length of the

Received 1 October 1998; revision received 25 February 1999; accepted for publication 25 June 1999.

*Senior Scientist; currently Aerospace Engineer, Mail Stop 396, Metals and Thermal Structures Branch, NASA Langley Research Center, Hampton, VA 23681. Senior Member AIAA.

†Astronaut, Mail Code CB, 2101 NASA Road. Associate Fellow AIAA.

§Retired, P.O. Box 1663, Mail Stop J576; currently Technical Staff Member, Comforce, Inc., Los Alamos, NM 87545.

‡Staff Member, Energy and Process Engineering, P.O. Box 1663, Mail Stop J576.

heat pipe. The heat pipe was tested in a vacuum chamber at Los Alamos National Laboratory (LANL) using induction heating. The heat pipe operated properly but failed prematurely due to electrical discharge between the induction heating concentrator and the heat pipe.

Results and Discussion

A single D-shaped cross section heat pipe in the shape of a leading edge was fabricated and tested at LANL. After fabrication, the heat pipe was tested at LANL using induction heating in a vacuum chamber. A discussion of the fabrication and testing follows.

Fabrication

Because of a relatively small leading-edge radius of 0.5 in., fabrication of the nose region of the heat pipe was challenging. The leading-edge-shaped, or J-tube, heat pipe had a D-shaped cross section but had only a short leg on one side of the nose region and a long leg on the opposite side of the nose region. Several techniques were evaluated to fabricate the nose region of the heat pipes. Bending the D-shaped tube to the desired radius was not found to be feasible, nor was bending sections and then welding the nose together. The technique that was finally utilized was to machine the nose components out of a solid piece of Mo–41Re and weld them together to form the nose region. A photograph of the two nose section pieces individually and welded together with the tubing on both sides is shown in Fig. 1. The end plugs and a cover to be placed over the fill tube are also shown in the photograph. The machining, tube drawing, and welding were performed by Thermo Electron Tecomet, Wilmington, Massachusetts.

The artery was fabricated by wrapping three layers of 400×400 mesh Mo–5Re screen around a 0.125-in.-outer-diameter steel mandrel and was held in place with a 0.003-in.-diam steel wire spirally wrapped the length of the artery. The steel mandrel/screen assembly was inserted into a 0.25-in.-outer-diameter by 0.035-in. wall steel sheath. The steel sheath was drawn down to a 0.210-in. outer diameter. After the final draw, the assembly was immersed in a water/hydrochloric solution, and the steel mandrel, sheath, and wire were dissolved leaving the formed screen artery.

The screen wick was fabricated by wrapping the first two layers of 400×400 mesh screen over a copper mandrel that had been machined to the wick's final shape. The artery was placed over the first two layers of screen, the final two layers of screen were wrapped over the mandrel and artery, and the edge of the final wrap was spot welded the length of the wick. The assembly was then slid off the copper mandrel.

Testing

After the heat pipe was assembled, 0.017 lb (7.5 g) of lithium was loaded into the heat pipe by distillation. The heat pipe was wet-in at 3170°F for 53 h in a vacuum furnace. After wet-in, the heat pipe was oriented with the short leg of the heat pipe on the top and the long leg on the bottom and placed in a vacuum test chamber. An rf-induction coil/concentrator was used as the heat source. The heating device was designed to heat the entire width of the flat portion of the heat pipe for a chord length of 1.6 in. in the nose region. Initial tests heated the heat pipe to 1700°F, resulting in a heat flux of approximately 362 Btu/ft^2-s.

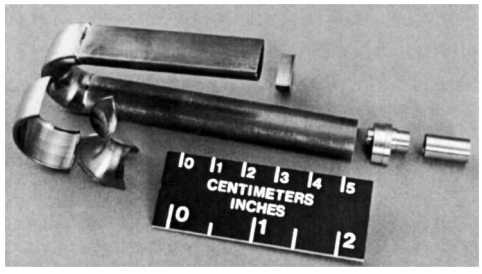

Fig. 1 Photograph of the individual machined nose components and the completed nose assembly with the end plugs and fill tube cover.

To put enough heat into the heat pipe to heat the entire heat pipe to operating temperatures, a large heat flux was required in the nose region. During initial testing of the heat pipe, the inside surface of the nose region remained hotter than the outside heated surface. The hot spot resulted because the inside surface was heated by the induction heating but was not adequately cooled by the liquid lithium. The heating distribution resulted from the nature of induction heating, which inductively heated the entire nose region. The inside surface of the nose region was not cooled adequately due to the discontinuous wick on that surface.[4] In the actual application, inadequate cooling of the inside surface would not be a problem because it would not be subject to the aerodynamic heating.

The approach taken to solve the hot spot problem was to insulate the inside, curved surfaces of the heat pipe. In actual operation, the inside surface would radiate only a minimal amount of heat. If the inside surface were insulated, then less heat input would be required to raise the heat pipe to operating temperatures. With less heating in the nose region, the inside surface of the nose region might not develop a hot spot.

The heat pipe was mounted inside the vacuum chamber with the nose region facing an rf concentrator and coils. RF power was induced from the coils to the concentrator and then to the heat pipe. Porous refractory insulation that had been baked for several days at 1880°F was placed on inward facing surfaces to reduce radiative coupling between the heat pipe and the chamber walls.

W/W–Re thermocouples were placed on the heat pipe by strapping them down with wire because prior experience welding thermocouples on a different Mo–Re heat-pipe container was unsuccessful.[2] Though the temperature uncertainty was greater than if the thermocouples were welded, the operation of the thin-walled heat pipe was not compromised by the instrumentation. Two thermocouples were located on the upper surface (the short leg), and six were located on the lower surface (long leg). The thermocouple locations for thermocouples 1–8 were, respectively, $s = 1.2$, -1.4, -3.5, 8.1, 14.9, 21.8, 28.7, and 30.7 in. The stagnation line is at $s = 0$ in., with negative numbers referring to the short leg on the upper surface.

Four tests were performed prior to catastrophic failure of the heat pipe. In each case, the heat pipe was started up over the course of several hours. Though neither isothermal nor design temperatures were obtained, the heat pipe was operational. The startup data from the second test are shown in Fig. 2. In this case, the heat flux was reduced after about 6 h and then increased again. Steady-state temperatures were then obtained. However, isothermal operation was not obtained due to the low heat fluxes required to minimize outgassing of the insulation. Because the thermocouples were strapped onto the heat pipe, the uncertainity of the readings is unknown. However, it is likely that the actual heat-pipe temperature was higher than the thermocouple reading.

In the first two tests, the heat pipe was operational over most of the entire length, whereas in the two later tests, it was operational only over a portion of the heat-pipe length, as shown in Fig. 3. The data in Fig. 3 show typical elevated temperatures obtained during each test but do not represent steady-state temperatures. The data for test 1 do not include a temperature at $s = 8.1$ in. because the thermocouple

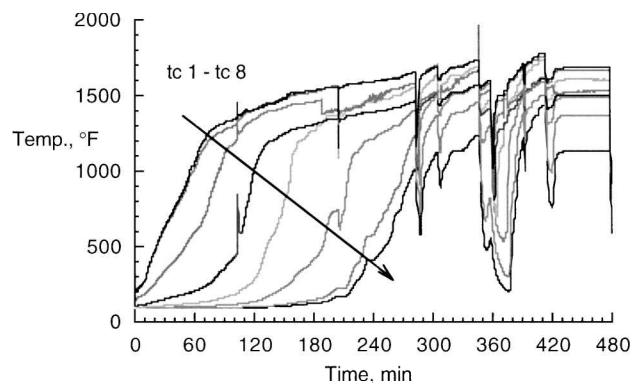

Fig. 2 Startup data for heat pipe during second test.

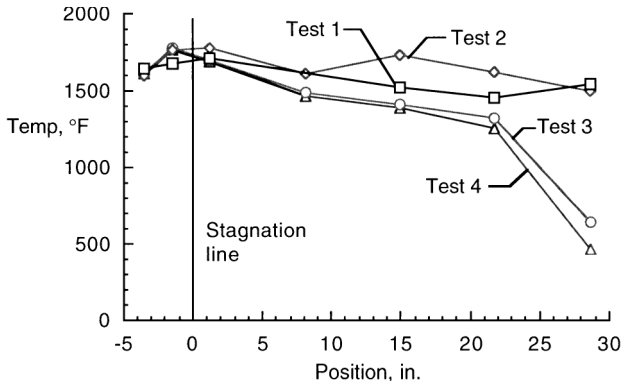

Fig. 3 Heat-pipe temperatures during the four tests.

was not functioning properly at the time. From Fig. 3, it is apparent that the leading-edge-shaped heat pipe did operate as expected, though design temperatures and heat fluxes were not obtained.

During the fourth and final test, the heat pipe was destroyed by an electrical discharge between the induction heating concentrator and the heat pipe. This unfortunate event was most likely precipitated by volatile outgassing from the refractory insulation.

Conclusion

A leading-edge-shaped Mo–Re heat pipe was fabricated and tested. Several container and wick fabrication issues were resolved that arose due to the small 0.5-in.-leading-edge radius. The heat pipe was tested in a vacuum chamber with induction heating. The heat pipe did start up as expected and operated as a heat pipe, however, not at design heat fluxes and temperatures. Though a testing anomaly caused premature failure of the heat pipe, successful startup and operation of the heat pipe are key steps toward the development of heat pipes for cooling sharp leading edges.

Acknowledgment

The authors would like to thank the Thermal Structures Branch at NASA Langley Research Center for funding this work under Contract NAS1-96014.

References

[1]Glass, D. E., and Camarda, C. J., "Preliminary Thermal/Structural Analysis of a Carbon–Carbon/Refractory-Metal Heat-Pipe-Cooled Wing Leading Edge," *Thermal Structures and Materials for High Speed Flight*, edited by E. A. Thornton, Vol. 140, Progress in Astronautics and Aeronautics, AIAA, Washington, DC, 1992, pp. 301–322.

[2]Glass, D. E., Camarda, C. J., Merrigan, M. A., and Sena, J. T., "Fabrication and Testing of Mo–Re Heat Pipes Embedded in Carbon/Carbon," *Journal of Spacecraft and Rockets*, Vol. 36, No. 1, 1999, pp. 79–86.

[3]Glass, D. E., Camarda, C. J., and Merrigan, M. A, Refractory-Composite/Heat-Pipe-Cooled Leading Edge, U.S. Patent 5,720,339, Feb. 1998.

[4]Glass, D. E., Merrigan, M. A., Sena, J. T., Reid, R. S., "Fabrication and Testing of a Leading-Edge-Shaped Heat Pipe," NASA CR-1998-208720, Oct. 1998.

H. L. McManus
Associate Editor